CYCLIC RESPONSE OF SMART SENSING LAYER FOR INSITU STRUCTURAL HEALTH MONITORING OF COMPOSITE MATERIALS

Zaffar M. Khan, Saad Nauman, Mohammad A. Walid

Department of Aeronautics and Astronautics, Institute of Space Technology, Islamabad, Pakistan

Department of Materials Science and Engineering, Institute of Space Technology, Islamabad, Pakistan

Department of Mechanical Engineering, University of Engineering & Technology, Taxila, Pakistan

ABSTRACT

In this paper we have investigated cyclic response of smart sensing layer deposited on GFRP substrate. The smart layer was composed of a thermoplastic matrix (High density Polystyrene) and a dispersed Nano-filler (Carbon Nano-particles). This is in continuation of our earlier work where we successfully demonstrated structural health monitoring capability of such smart layers. Cyclic tests were performed to demonstrate the repeatability of the sensor as well as various characteristics such as, linearity, saturation and general response characteristics. The substrate chosen was glass fiber laminated composite comprising of 8 layers of woven fabric reinforcements fabricated using VARTM technique. The smart sensing layer was deposited on the composite specimens in the center using doctor blade and a slot die. The dynamic response of the smart layer reveals that the sensors are able to follow loading and unloading cycles without any delay. The response of the sensor is frequency dependent with saturation / noise observed at high frequency cyclic testing. The smart layer also demonstrates repeatability when cyclic loads are applied.

1. INTRODUCTION

In recent times industry has witnessed wide application of high strength composite materials especially in the areas of aerospace, auto-motives, civil engineering and sports/leisure etc. Their success in these fields has been due to their exceptional mechanical properties and a mix of supplementary traits such as corrosion resistance, shaping ability and parts consolidation etc. For reliable use of composite materials their design schemes should be well understood and maintenance procedures should be developed. Maintenance requires inspection which is generally scheduled in case of traditional metal parts where damage has limited types and causes. On the other hand

Copyright 2019. Used by the Society of the Advancement of Material and Process Engineering with permission.

SAMPE Conference Proceedings. Charlotte, NC, May 20-23, 2019. Society for the Advancement of Material and Process Engineering – North America.

due to the anisotropic nature of fiber reinforced composite materials damage can occur and propagate in a number of ways. As a consequence scheduled inspection might be too late to avoid the loss of life and property. Continuous monitoring of composite parts during their service life is one possible solution to this problem. In service structural health assessment of FRPs enhances operational reliability by providing means for safe operating conditions. It might be said therefore, that the development of cost effective on-line structural health monitoring schemes is the need of the hour.

The use of different sensing mechanisms has been thoroughly researched and reviewed in literature. Acoustic Emission, X-ray Tomography, Fiber Bragg Gratings, Digital Image Correlation have been reported as structural health and integrity monitoring methods (Unnthorsson et al., 2008; Fu et al., 2009; Panopoulou et al., 2011; Naderi et al., 2012; Hamdi et al., 2013; Wang et al., 2013).

The use of smart materials as sensing members of the structure has also been investigated as an alternative structural health monitoring method. Exploiting electrical properties of materials has proven to be a useful tool of making a material sensitive to load or strain. For instance electrical response in relation to an applied strain or deformation can be monitored in real time for extracting useful information about a structure's health (Swait et al., 2012). Carbon based smart materials owing to their strength and piezoresistive properties can be used to make strain gauges with gauge factors exceeding those of traditional metal foil types. These strain sensors are widely reported to provide useful information about the mechanism of failure of composites in cyclic loading above and below the strength level of material (Okuhara and Matsubara, 2007; Chung, 2012; Ku-Herrera and Avilés, 2012; Materazzi et al., 2013).

Conductive nano fillers of carbon such as CNPs, CNTs and Graphene Nano Platelets can be used in conjunction with a suitable matrix to enhance conductivity up to appreciable levels (Sohi et al., 2011; Pham et al., 2008). For carefully maintained concentration levels these composites can be made piezoresistive owing to the tunneling effect at percolation threshold of the nano filler (Knite and Linarts, 2015; Vertuccio et al., 2015; Nauman et al., 2011b; Nauman et al., 2011a; Nauman et al., 2012; Nasir et al., 2014). Incorporation of such fillers in a suitable thermoplastic or an elastomer can result in composites which can serve as sensors when attached to the target substrate just like a metal foil strain gauge. The main advantages of such smart gauges for strain sensing are their low cost, ability to engineer properties/geometry and their exceptionally high sensitivities/Gauge factors (Hu et al., 2008; Hierold et al., 2007).

Smart composites have been a subject of intensive academic research. Many different approaches have been investigated in this regard. Among these Fiber Brag Grating sensors (Maaskant et al., 1997; Murukeshan et al., 2000; Panopoulou et al., 2011; Takeda et al., 2005) (Zheng et al., 2014)and use of nano fillers for in situ monitoring of composites (Nauman et al., 2011a; Nauman et al., 2012; Nauman et al., 2011b; Nasir et al., 2014) appear to be the forerunners as far as composite structures are concerned.

Different aspects of these smart composites have been investigated recently. Zheng et al. (Zheng et al., 2014) reported the behavior of polymer matrix composites (PMCs) with HDPE as the matrix and Carbon Black as the filler material at percolation threshold under low number of tensile cycles. The effect of maximum applied strain on residual resistance of GFRP/CB composites has also been studied (Okuhara and Matsubara, 2007) and it was found that residual resistance of composite structures can be used to determine previously applied maximum strain. The behavior of CB/Polypropylene and CNT/Polypropylene composites under cyclic tensile loading was discussed by (Zhao et al., 2013). They proposed possible reasons for different behaviors of CB/Polypropylene and CNT/Polypropylene composites. According to their findings, in CNT/PP, due to gradual loading and unloading, a better conductive network was developed owing to hysteresis effect which is the direct result of visco-elastic nature of composite materials.

The present work investigates the behavior of PS/CB smart coatings under cyclic loading for on-line in-situ structural health monitoring. This smart coating has already been investigated under monotonic loading in one of our earlier research works (Nasir et al., 2014).

2. EXPERIMENTATION

2.1 Preparation of smart sensing layer

High density polystyrene was selected as the matrix material whereas Carbon Nano-particles supplied by Degussa were used as Nano-particles. These particles have spherical geometry and their average diameter is reported to be 50 nm. It has been found through repeated and systematic investigations that when weight concentration of these particles is maintained at 35% the resulting polymer matrix composite becomes piezoresistive (Nauman et al., 2011b; Cochrane et al., 2010) since the said concentration pertains to the percolation threshold of these Nano-particles in the polystyrene.

The dispersion was prepared by adding Polystyrene and Carbon Nano-particles in benzene solvent. The mixture was stirred overnight to allow Nano-particles to disperse thoroughly in the matrix.

2.2 Fabrication of composite specimens

The composite substrate chosen for the purpose of smart layer deposition were laminated structures comprising of 8 plies of plain woven glass fabric supplied by Interglas Technologies Gmbh (Interglas 92110). The epoxy resin used was Araldite LY5052 with hardener Aradur 5052 supplied by Huntsman®. The process used was vacuum assisted resin transfer molding (VARTM). In this way sheets of composite laminates were prepared.

2.3 Specimen geometry

The sheets of composite laminates were cut into rectangular specimens using Metacut M-350. Thereafter smart sensing layer was deposited in the middle of these specimens (described in the next section). The exact dimensions of composite specimens along with the length of deposited smart layers have been reported in table 1.

Table 1. Specimens' geometric parameters

Specimen No	Specimen Width (mm)	Specimen length (cm)	Thickness (mm)	Smart layer length (mm)
1	25.3	24.9	1.05	10
2	25.3	24.9	1.14	12.3
3	25.8	24.9	1.10	11.54
4	25.7	24.95	1.07	12.32
5	25.5	24.95	1.10	12.81
6	25.1	24.95	1.11	12.91

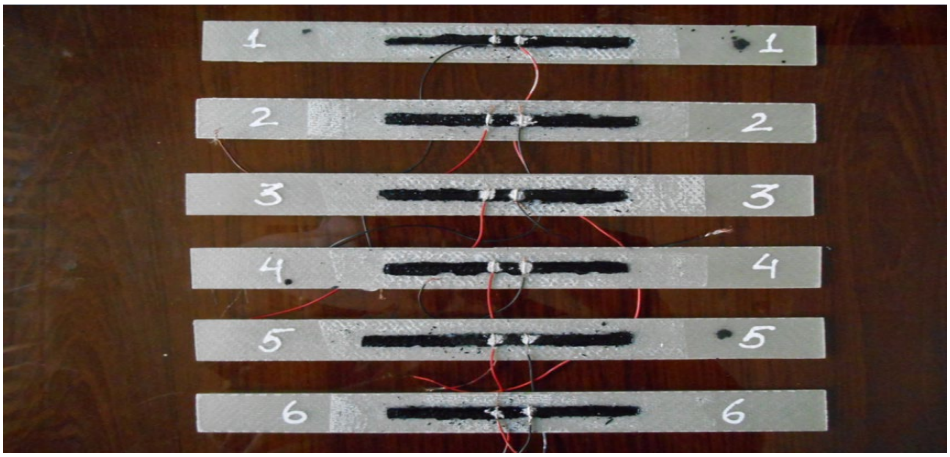


Figure 1. Specimens with smart coating and conductive silver paint connections

2.4 Deposition of smart layer

The smart layer was deposited in the middle of the specimen surface using doctor blade technique while employing a slot die of the dimensions roughly equal to that of the intended smart layer. The deposited smart layer is shown in Figure 1. The exact dimensions of these layers, after deposition on different specimens are reported in table 1.

2.5 Data acquisition and filtering

Commercially available data acquisition module, KUSB 3100 was used for the purpose of data acquisition. For data amplification an instrumentation amplifier INA101 was employed. The unknown resistance of the smart sensing layer was connected in Wheatstone configuration. Moreover low pass filters also helped reduce noise in the sensor output.

3. EXPERIMENTAL METHODOLOGY

These specimens were mounted on MTS 810 for cyclic tensile loading as shown in Figure 2.

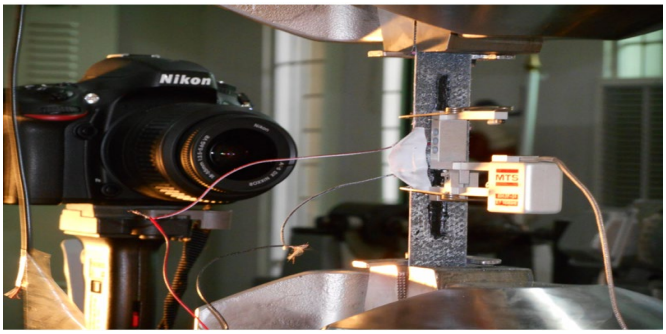


Figure 2. Specimen Mounted on MTS 810 with Extensometer and electrical connections

A maximum load of 25% of the breaking load was applied in the cyclic configuration. The 25% breaking load applied, corresponds to 120 MPa testing load. Total number of cycles were kept 20 for all the tests. The frequencies were adjusted to achieve a specific strain rate in the gauge length. Table 2 gives all the strain rates and the corresponding loading frequencies along with the initial force and amplitude of cyclic loading.

Table 2. Testing parameters adopted for cyclic tests

Specimen No.	Strain rate mm/min	Frequency (Hz)	Initial force (MTS 810) KN	Amplitude (mm)	No of cycles
1	5	0.17	0.63	0.25	20
2	10	0.34			
3	50	1.70			
4	100	3.40			
5	200	6.80			
6	400	17.6			

4. RESULTS & DISCUSSION

The testing is done for two load values (to be quoted here) at 6 different strain rates (refer to Figure 3).

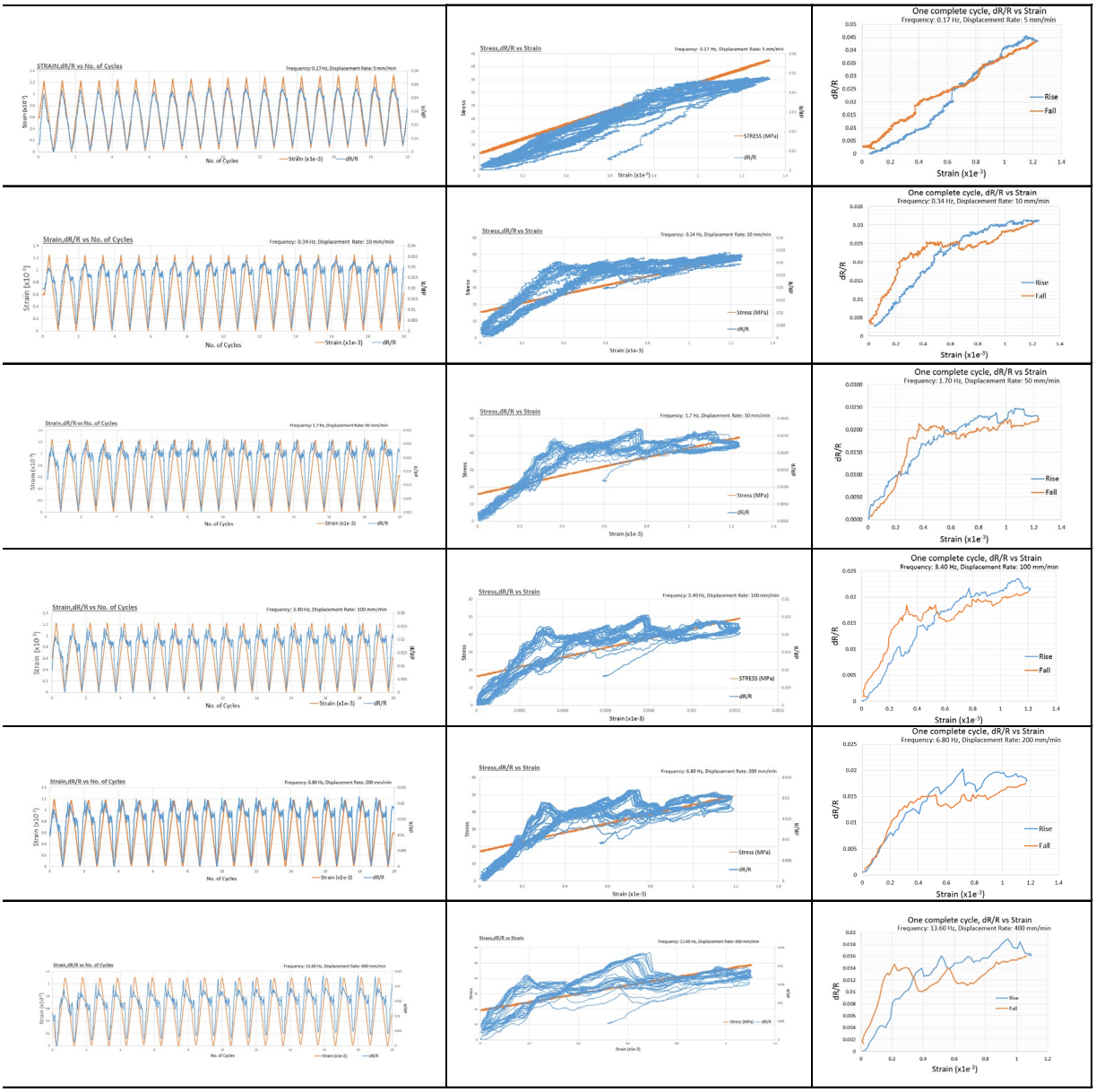


Figure 3. Cyclic response of smart layer composites at different strain rates (a) 5 mm/min, (b) 10 mm/min, (c) 50 mm/min, (d) 100 mm/min, (e) 200 mm/min, (f) 400 mm/min

The results show that the sensors respond well to the applied load / strain. Three main quantities were evaluated for these sensors. The first one was the general cyclic response of the sensor against the strain produced in the specimen at different frequencies. To be noted is that the specimens have been tested in a load controlled experiment and a slight creep of the specimen is witnessed. The sensor response follows well this creep in deformation. In Figure 3(a) the frequency is slow at 0.17 Hz. The tendency of the specimen to creep is higher. One can see that during the cycling the maximum strain increases by about 13%. The response of the sensor also increases by the same amount. One can also remark that for the first few cycles the response is very sharp. After about 4-5 cycles the high stress part of the cycle starts to show some noise. This peak noise has some interesting characteristics. It appears for all the strain rates except for the very high strain rate testing (refer to Figure 5(f)). The second interesting characteristic is that this noise is present at the peak load only. It creates a sort of dwell or saturation of the sensor response. Of particular interest is the fact that due to this dwell, the slope of sensor response, (rise and fall of the sensor signal) is altered, so as to accommodate this dwell at peak load. This dwell remains remarkably symmetric to the strain response.

Since the specimens are made of viscoelastic material, high strain rates give smaller absolute strain values, for the same load. It is thus seen that the sensor has a deformation limit, upto which it gives a linear response. Beyond this limit, the dwell and noise start to appear as is evident from Figure 3. From these results it can be inferred that the saturation level of the sensor changes with the increase in deformation rate (upper limit is reduced). The graph plotted in Figure 4 defines the limit of response for this smart sensing layer. The area lower than the curve represents the effective range of the sensor with respect to the applied strain rates. The loss of sensor range is of the order of 250% in the tested range of frequencies.

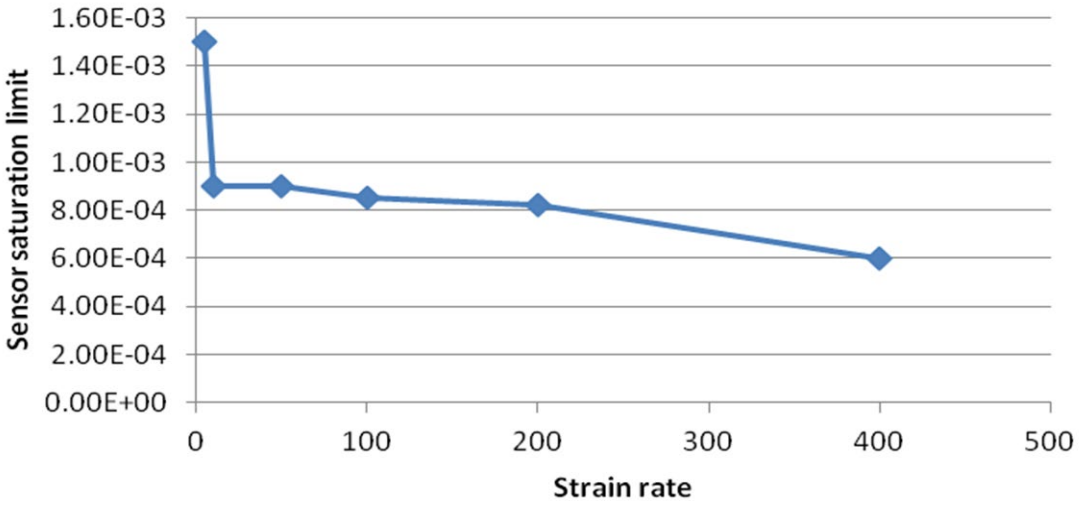


Figure 4. Limit of response for the smart sensing layer under cyclic loading

The loading and unloading curves of the sensor represent another interesting characteristic. The rising and falling curves are more or less coincident, with better coincidence for higher strain rates. At lower strain rates the difference between the two curves is more pronounced. However, the end points of the curves (max and min strain) match perfectly (Figure 3). The difference in loading and unloading does not seem to be maximum strain range dependent. The knee in the curves is due to the maximum strain saturation limit achieved at higher loads.

The cyclic response and load-unload response leads us to believe that the max strain range limit is actually dependent on the material of the sensor. The viscoplastic behavior of the PS used for the sensor material will change with increase in deformation rate. Since the sensor works on the effect of tunneling and breakage of conductivity networks due to tensile loading, a difference in the deformation characteristics of the PS would strongly influence the sensor response. This is particularly obvious in the slowest deformation rate (Figure 3(a)). The first cycle is perfect with respect to sensor response. However, due to cycling, it cannot be assured that the PS will maintain a constant response to the applied load or strain. Cyclic hardening or softening of the sensor material may modify the sensor response to a great degree. This is seen that at the last cycle the sensor measurement range has changed considerably. At higher cycling rates the response stabilizes more quickly and remains constant (Figure 3(f)).

The hysteresis curves show that the sensors show some hysteresis at all deformation rates. Higher noise in the cyclic response corresponds to the higher hysteresis in response. (refer to Figure 3(a) as an instance of slow cycling rate and Figure 3(f) as that of fast cycling rate).

5. CONCLUSIONS

The results demonstrate that the smart sensing layer developed and applied on composite specimens can be used for monitoring structural vibrations, mechanical excitation and cyclic loads. The coating remained intact within a safe strain limit and showed no physical damage after 20 cycles. It is clear that the resistivity change is in adequate agreement with the strain.

Further study of the large strain sensing ability of the smart sensing layer is focused at increasing the bandwidth of the dynamic response, minimization or correction of resistance drift and determination of the long term reliability of the sensor material.

Conflict of Interest

Authors declare that there is no conflict of interest.

Funding Sources

This research work has been performed as part of joint research as part of PhD program at University of Engineering and Technology, Taxila and Institute of Space Technology, Islamabad, Pakistan.

6. REFERENCES

1. Chung DDL. (2012) Carbon materials for structural self-sensing, electromagnetic shielding and thermal interfacing. *Carbon* 50: 3342-3353.

2. Cochrane C, Lewandowski M and Koncar V. (2010) A flexible strain sensor based on a conductive polymer composite for in situ measurement of parachute canopy deformation. *Sensors* 10: 8291-8303.

3. Fu T, Liu Y, Li Q, et al. (2009) Fiber optic acoustic emission sensor and its applications in the structural health monitoring of CFRP materials. *Optics and Lasers in Engineering* 47: 1056-1062.

4. Hamdi SE, Le Duff A, Simon L, et al. (2013) Acoustic emission pattern recognition approach based on Hilbert–Huang transform for structural health monitoring in polymer-composite materials. *Applied Acoustics* 74: 746-757.

5. Hierold C, Jungen A, Stampfer C, et al. (2007) Nano electromechanical sensors based on carbon nanotubes. *Sensors and Actuators A: Physical* 136: 51-61.

6. Hu N, Karube Y, Yan C, et al. (2008) Tunneling effect in a polymer/carbon nanotube nanocomposite strain sensor. *Acta Materialia* 56: 2929-2936.

7. Knite M and Linarts A. (2015) Polymer/Nanographite Composites for Mechanical Impact Sensing. *Graphene-Based Polymer Nanocomposites in Electronics.* Springer, 223-252.

8. Ku-Herrera JJ and Avilés F. (2012) Cyclic tension and compression piezoresistivity of carbon nanotube/vinyl ester composites in the elastic and plastic regimes. *Carbon* 50: 2592-2598.

9. Maaskant R, Alavie T, Measures R, et al. (1997) Fiber-optic Bragg grating sensors for bridge monitoring. *Cement and Concrete Composites* 19: 21-33.

10. Materazzi AL, Ubertini F and D'Alessandro A. (2013) Carbon nanotube cement-based transducers for dynamic sensing of strain. *Cement and Concrete Composites* 37: 2-11.

11. Murukeshan V, Chan P, Ong L, et al. (2000) Cure monitoring of smart composites using fiber Bragg grating based embedded sensors. *Sensors and Actuators A: Physical* 79: 153-161.

12. Naderi M, Kahirdeh A and Khonsari MM. (2012) Dissipated thermal energy and damage evolution of Glass/Epoxy using infrared thermography and acoustic emission. *Composites Part B: Engineering* 43: 1613-1620.
13. Nasir MA, Akram H, Khan ZM, et al. (2014) Smart sensing layer for the detection of damage due to defects in a laminated composite structure. *Journal of Intelligent Material Systems and Structures*: 1045389X14554138.

14. Nauman S, Cristian I and Koncar V. (2011a) Simultaneous application of fibrous piezoresistive sensors for compression and traction detection in glass laminate composites. *Sensors* 11: 9478-9498.

15. Nauman S, Cristian I and Koncar V. (2012) Intelligent carbon fibre composite based on 3D-interlock woven reinforcement. *Textile Research Journal* 82: 931-944.

16. Nauman S, Lapeyronnie P, Cristian I, et al. (2011b) Online measurement of structural deformations in composites. *Sensors Journal, IEEE* 11: 1329-1336.

17. Okuhara Y and Matsubara H. (2007) Carbon-matrix composites with continuous glass fiber and carbon black for maximum strain sensing. *Carbon* 45: 1152-1159.

18. Panopoulou A, Loutas T, Roulias D, et al. (2011) Dynamic fiber Bragg gratings based health monitoring system of composite aerospace structures. *Acta Astronautica* 69: 445-457.

19. Pham GT, Park Y-B, Liang Z, et al. (2008) Processing and modeling of conductive thermoplastic/carbon nanotube films for strain sensing. *Composites Part B: Engineering* 39: 209-216.

20. Sohi NJS, Bhadra S and Khastgir D. (2011) The effect of different carbon fillers on the electrical conductivity of ethylene vinyl acetate copolymer-based composites and the applicability of different conductivity models. *Carbon* 49: 1349-1361.

21. Swait TJ, Jones FR and Hayes SA. (2012) A practical structural health monitoring system for carbon fibre reinforced composite based on electrical resistance. *Composites Science and Technology* 72: 1515-1523.

22. Takeda N, Okabe Y, Kuwahara J, et al. (2005) Development of smart composite structures with small-diameter fiber Bragg grating sensors for damage detection: Quantitative evaluation of delamination length in CFRP laminates using Lamb wave sensing. *Composites Science and Technology* 65: 2575-2587.

23. Unnthorsson R, Runarsson TP and Jonsson MT. (2008) Acoustic emission based fatigue failure criterion for CFRP. *International Journal of Fatigue* 30: 11-20.

24. Vertuccio L, Vittoria V, Guadagno L, et al. (2015) Strain and damage monitoring in carbon-nanotube-based composite under cyclic strain. *Composites Part A: Applied Science and Manufacturing*.

25. Wang P, Takagi T, Takeno T, et al. (2013) Early fatigue damage detecting sensors—A review and prospects. *Sensors and Actuators A: Physical* 198: 46-60.

26. Zhao J, Dai K, Liu C, et al. (2013) A comparison between strain sensing behaviors of carbon black/polypropylene and carbon nanotubes/polypropylene electrically conductive composites. *Composites Part A: Applied Science and Manufacturing* 48: 129-136.

27. Zheng S, Deng J, Yang L, et al. (2014) Investigation on the piezoresistive behavior of high-density polyethylene/carbon black films in the elastic and plastic regimes. *Composites Science and Technology* 97: 34-40.